

Classical Theory of Quantum Work Distribution in Chaotic Fermion Systems

András Grabarits,^{1,2} Márton Kormos,² Izabella Lovas,^{3,4} and Gergely Zaránd^{1,2}

¹*BME-MTA Exotic Quantum Phases ‘Lendület’ Research Group, Institute of Physics, Budapest University of Technology and Economics, Budafoki út 8., H-1111 Budapest, Hungary*

²*MTA-BME Quantum Dynamics and Correlations Research Group, Institute of Physics, Budapest University of Technology and Economics, Budafoki út 8., H-1111 Budapest, Hungary*

³*Department of Physics and Institute for Advanced Study, Technical University of Munich, 85748 Garching, Germany*

⁴*Munich Center for Quantum Science and Technology (MCQST), Schellingstr. 4, D-80799 München*

(Dated: July 22, 2021)

We present a theory of quantum work statistics in generic chaotic, disordered Fermi liquid systems within a driven random matrix formalism. By extending P. W. Anderson’s orthogonality determinant formula to compute quantum work distribution, we find that work statistics is non-Gaussian and is characterized by a few dimensionless parameters. At longer times, quantum interference effects become irrelevant and the quantum work distribution is well-described in terms of a purely classical ladder model with a symmetric exclusion process in energy space, while bosonization and mean field methods provide accurate analytical expressions for the work statistics. Our random matrix and mean field predictions are validated by numerical simulations for a two-dimensional disordered quantum dot, and can be verified by calorimetric measurements on nanoscale circuits.

Introduction.— The concepts of heat and work lie at the foundations of thermodynamics and statistical physics. When considered in the quantum realm, however, they raise deep questions and pose new challenges [1]. Even the very definitions of heat and energy transfer become nontrivial as they require the specification of the measurement protocol [2]. At the same time, the interplay of quantum and thermal fluctuations, coherence, and dissipation gives birth to novel phenomena which are in the focus of the rapidly growing field of quantum thermodynamics connecting quantum physics, thermodynamics, and quantum information theory [4, 5]. With the recent experimental developments, these issues are not purely academic but can be studied in the laboratory, in systems ranging from individual molecules [6–8] through mesoscopic grains [9, 10] and nuclear spins [11] to cold atoms [12] and nitrogen vacancy centers [13].

The definition and measurement of work in quantum systems requires a two-time measurement protocol: one first determines the energy E_0^i of the initial state at time $t = 0$, and later, in a second measurement, the energy E_t^f of the time evolved system at time t . The adiabatic part being essentially trivial, here we focus on the ‘entropic’ contribution of energy absorption or ‘work’, defined as $W \equiv E_t^f - E_0^i$, i.e., the energy absorbed ($W > 0$) or emitted ($W < 0$) by the system due to non-adiabatic transitions, and investigate the corresponding distribution function, $P_t(W)$. The full distribution of work has been studied extensively in many-body systems [14–20], and its characteristic function of this distribution has been related to the Loschmidt echo [14, 21] and to quantum information scrambling [21]. However, the effect of disorder and randomness is much less studied [22–24] despite their relevance in mesoscopic systems.

To fill this gap, here we focus on disordered, chaotic

fermion systems such as 2-dimensional quantum dots, which we perturb by changing external gate voltages, fields, and electrodes, as shown in Fig. 1.a. We neglect interactions under the assumptions that a non-interacting Fermi liquid description is appropriate. Under these conditions, the system can be described in terms of the time

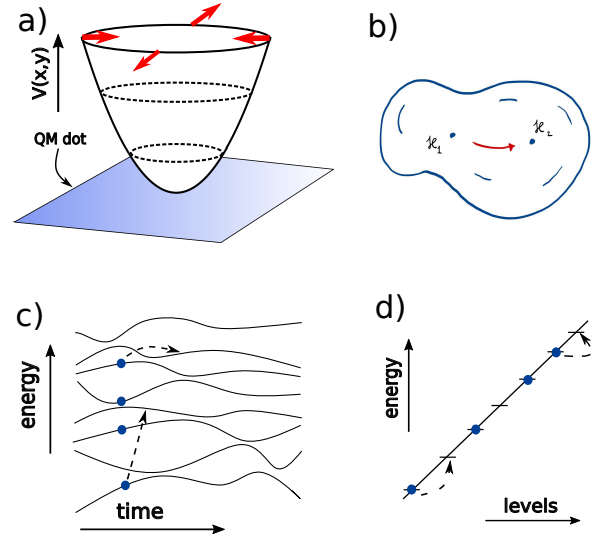


FIG. 1. a) Disordered 2-dimensional electron gas with a parabolic potential deformed in time, driving the system away from equilibrium. b) Motion in the manifold of random matrices. c) Deformation-induced motion of energy levels, giving rise to particle-hole excitations. d) ‘Ladder’ model: classical diffusion of hard core particles between uniformly spaced energy levels.

dependent Hamiltonian

$$\hat{H}(t) = \sum_{i,j=1}^N \hat{a}_i^\dagger \mathcal{H}_{ij}(t) \hat{a}_j, \quad (1)$$

where the \hat{a}_i 's stand for fermionic annihilation operators, and the single particle Hamiltonian $\mathcal{H}(t)$ incorporates disorder effects and also accounts for the impact of time dependent electrodes. The total fermion number is conserved by Eq. (1), $\sum_i \hat{a}_i^\dagger \hat{a}_i = M$. For a concrete physical system such as a quantum dot defined in a disordered 2 dimensional electron gas, we can and will construct microscopic models for $\mathcal{H}(t)$ and compute work statistics. The single particle spectrum of most chaotic systems is, however, known to be captured by random matrix theory [25, 26]. We can therefore also follow the strategy of Refs. [27] and [28], and consider deformations within the space of Gaussian random matrix ensembles,

$$\mathcal{H}(t) = \mathcal{H}_1 \cos \lambda(t) + \mathcal{H}_2 \sin \lambda(t),$$

with $\mathcal{H}_{1,2}$ some independent $N \times N$ Gaussian matrices from the orthogonal (GOE), unitary (GUE) or symplectic (GSE) ensembles, and $\dot{\lambda} = v$ setting the speed of deformations. In this latter case, the parameter λ generates a motion along an 'arc' or 'circle' within the random matrix ensemble, as depicted in Fig. 1.b.

Our goal is to understand universal aspects of the structure and time evolution of the distribution $P_t(W)$. For simplicity, here we focus on *quantum quench* protocols, i.e., we start from the ground state of $\hat{H}(0)$, but our results can be readily generalized to finite temperature mixed states [29]. We follow the quantum evolution of the disordered many-body systems, and use a determinant formula presented in Ref. [28] to compute $P_t(W)$. We find that the statistics of $P_t(W)$ is almost independent of microscopic details as well as the symmetry of the Hamiltonian, once the absorbed energy exceeds sufficiently the one-body energy separation $\delta\epsilon \equiv 1/N(\epsilon_F)$, characterizing the total density of levels at the Fermi energy ϵ_F , and the time is long enough, $t > \hbar/\delta\epsilon$. To capture work in this long time limit, we construct a classical 'ladder' model which incorporates quantum statistics as well as level repulsion, but ignores interference effects between consecutive level collisions and Landau-Zener transitions. Our 'ladder' model gives a surprisingly accurate description of $P_t(W)$, and allows us to derive accurate analytical approximations for $P_t(W)$ by means of bosonization and a particle number conserving mean field method. We also validate the RMT description and the 'ladder' model in a 2D quantum dot system.

Quantummechanical analysis.— Since the Hamiltonian H is non-interacting, all information is contained in the time evolution of the single particle wave functions, $\varphi^m(t)$. These can be obtained by expanding $\varphi^m(t)$ in terms of the instantaneous eigenfunctions η_t^k of \mathcal{H} , as

$\varphi^m(t) = \sum_k \alpha_k^m(t) \eta_t^k$, and then solving the single particle Schrödinger equation for $\alpha_k^m(t)$. The generating function $G_t(u)$ of the work distribution $P_t(W)$ can then be expressed by a simple determinant formula ($\hbar = 1$) [28, 30]

$$\begin{aligned} G_t(u) &= \langle \langle \Psi(t) | e^{iu(\hat{H}(t) - E_{\text{GS}}(t))} | \Psi(t) \rangle \rangle_{\text{RM}} \\ &= \langle e^{-iu \sum_{m=1}^M \epsilon_m(t)} \det g_t(u) \rangle_{\text{RM}}, \end{aligned} \quad (2)$$

where the matrix $g_t(u)$ contains information on overlaps and the instantaneous single particle energies $\epsilon_k(t)$ at time t , $[g_t(u)]^{mm'} \equiv \sum_k [\alpha_k^m(t)]^* e^{iu\epsilon_k(t)} \alpha_k^{m'}(t)$. We compute $g_t(u)$ numerically, average over disorder or the random matrix ensemble, $\langle \dots \rangle_{\text{RM}}$, and determine the final distribution by performing a Fourier transformation.

The spacing $\delta\epsilon$ and its inverse provide natural energy and time scales, and allow us to introduce the dimensionless work and time, $w \equiv W/\delta\epsilon$ and $\tilde{t} \equiv t\delta\epsilon$, respectively. As shown in Fig. 1.c, deformations of the Hamiltonian lead to a continuous motion of single particle levels, and thereby induce collisions and transitions between them. These collisions and Landau-Zener transitions give rise to a *diffusive* broadening of the Fermi surface at longer times, where – after a short time perturbative $\sim t^2$ scaling – the average work is found to increase as $\langle w \rangle = \tilde{D}\tilde{t}$ with \tilde{D} the dimensionless energy diffusion constant (see Refs. [31] and [28]).

The distribution $P_{\tilde{t}}(w)$ can be disentangled into an adiabatic and a regular part,

$$P_{\tilde{t}}(w) = P_{\text{ad}}(\tilde{t}) \delta(w) + P_{\text{reg}}(w; \tilde{t}). \quad (3)$$

Random matrix theory implies that – apart from the symmetry of the Hamiltonian – the statistics of the evolution of the eigenvalues, sketched in Fig. 1.c, is completely characterized by the *velocity* with which levels deform, i.e., the frequency of avoided level crossings. Indeed, the average distance of level crossings, $\langle \Delta\lambda \rangle$ and the time scale $1/\delta\epsilon$ define a natural 'velocity' in parameter space, $v_c \equiv \langle \Delta\lambda \rangle \delta\epsilon$, which we can use to introduce the dimensionless velocity, $\tilde{v} \equiv \dot{\lambda}/(\langle \Delta\lambda \rangle \delta\epsilon)$ [32]. The dimensionless velocity characterizes microscopic processes. For $\tilde{v} \ll 1$ the motion is almost adiabatic, and small probability Landau-Zener transitions dominate. For $\tilde{v} \gg 1$, on the other hand, transitions between remote levels generate energy absorption.

From our random matrix considerations it follows that the distribution $P_{\tilde{t}}(w)$ can only depend on \tilde{t} , \tilde{v} , and, in case of finite temperature initial states, on the dimensionless initial temperature, $\tilde{T} \equiv T/\delta\epsilon$. Similarly, the diffusion constant \tilde{D} is a universal function of \tilde{v} , which scales as $\tilde{D} \sim \tilde{v}^2$ for large velocities, while for $\tilde{v} < 1$ nearest neighbor transitions dominate and yield $\tilde{D} \sim \tilde{v}^{(\beta/2+1)}$, with $\beta = 1, 2$ and 4 characterizing the orthogonal, unitary, and symplectic ensembles, respectively (see the Supplementary Material [31]).

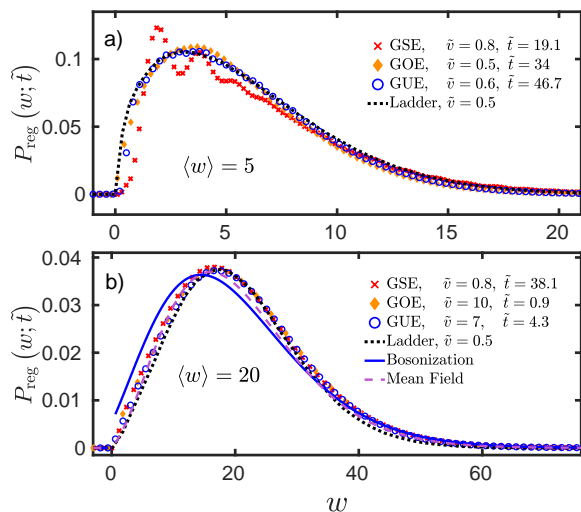


FIG. 2. Work statistics for GOE, GUE, GSE, for dimensionless average work $\langle w \rangle = 5$ (a), and $\langle w \rangle = 20$ (b). For smaller $\langle w \rangle$, $P_{\text{reg}}(w; \tilde{t})$ displays features associated with level repulsion and specific to the symmetry of the underlying Hamiltonian, while for large $\langle w \rangle$, the distributions $P_{\text{reg}}(w; \tilde{t})$ fall onto a single curve for all universality classes. Mean field (dashed line) and bosonization (continuous line) approaches give accurate description in the diffusive regime.

For small work, $\langle w \rangle \lesssim 10$, the statistics depends on β as well as on \tilde{v} and $P_{\text{reg}}(w; \tilde{t})$ displays peaks and minima associated with level repulsion, clearly reflecting the symmetry of the underlying Hamiltonian (see Fig. 2.a). For larger works, $\langle w \rangle \gtrsim \max\{\tilde{v}^2, 1\}$, however, one enters a diffusion dominated regime, where symmetry related and microscopic features become less important, and a universal distribution displayed in Fig. 2.b emerges. The observed distribution is clearly non-Gaussian, and characterizes work statistics in generic fermion systems.

Ladder model.— The agreement between the three universality classes is suggestive that quantum interference effects do not play an important role in this diffusion-dominated regime. We can therefore attempt and construct a classical ‘ladder’ model, consisting of uniformly placed classical energy levels at a distance $\delta\epsilon$ from each other,

$$\epsilon_k = k \delta\epsilon, \quad k = 1, 2, \dots, \quad (4)$$

occupied by hard core particles in line with Fermi statistics. The energy of a many-body state is then given by $E = \sum_k n_k \epsilon_k$ with $n_k \in \{0, 1\}$ the occupation numbers, and $\sum_k n_k = M$ the total number of particles. The evenly placed levels (4) mimic level repulsion and level rigidity in chaotic systems. As a final component, perturbation-induced random Landau–Zener transitions are modeled by nearest neighbor hopping transitions and a symmetrical exclusion process (SEP) in energy space. This simple model captures the diffusive broadening of the Fermi surface (see Ref. [31]) and, in addition to level

repulsion, it also incorporates Fermi statistics and particle number conservation. As can be seen in Figs. 2 and 3, this classical stochastic model gives a surprisingly accurate description of the work statistics for large enough average work, independently of the velocity. Moreover, with certain assumptions, the ‘ladder’ model can be used to compute $P_{\text{ad}}(\tilde{t})$ and $P_{\text{reg}}(w; \tilde{t})$ analytically for a $T = 0$ temperature initial state, without performing the actual Monte Carlo simulations, using either bosonization or a more accurate mean field approach. It is, however, crucial to treat particle number conservation with care.

Bosonization.— Bosonization offers a simple method to treat particle number conservation in the ‘ladder’ model. Introducing fermion operators for each level, we can express the total energy as $H = \sum_k (\epsilon_k - \epsilon_F) : c_k^\dagger c_k :$ with $\epsilon_F = \delta\epsilon(M + 1/2)$ the Fermi energy and $: \dots :$ referring to normal ordering with respect to the Fermi sea. Following Ref. [33], we introduce bosonic operators, $b_{q>0}^\dagger \equiv (1/\sqrt{q}) \sum_k c_{k+q}^\dagger c_k$, which satisfy the usual commutation relations, $[b_q, b_{q'}^\dagger] = \delta_{q,q'}$, and rewrite the Hamiltonian in terms of these as

$$H = \sum_{q \in \mathbb{Z}^+} \delta\epsilon q b_q^\dagger b_q + \frac{\delta\epsilon}{2} \hat{N}^2 \quad (5)$$

with $\hat{N} = \sum_k c_k^\dagger c_k - M$ the normal ordered fermion number. Clearly, the fermion number does not change for the closed system studied here so the second term in Eq. (5) does not give a contribution. We can obtain an approximate expression for $P_{\tilde{t}}(w)$ by assuming that the final state is thermal with an effective boson temperature $\tilde{T}_{\text{eff}} = \sqrt{6\langle w \rangle}/\pi$, chosen to yield the appropriate average energy, $\langle \sum_{q>0} b_q^\dagger b_q \rangle \equiv \langle w \rangle$. In the large $\langle w \rangle$ limit, we then obtain (see [31]),

$$P_{\tilde{t}}^{\text{Bose}}(w) \approx e^{-\frac{\pi^2 \tilde{T}_{\text{eff}}}{6}} \left[\frac{\pi}{\sqrt{6} w} e^{-w/\tilde{T}_{\text{eff}}} I_1(\pi \sqrt{\frac{2}{3}} w) + \delta(w) \right], \quad (6)$$

where I_1 is the modified Bessel function of the first kind. Since $T_{\text{eff}} \sim \sqrt{D\tilde{t}}$, the prefactor decays as $\sim e^{-C\sqrt{D\tilde{t}}}$, corresponding to a stretched exponential decay of adiabatic processes, as confirmed by our quantum mechanical simulations [28].

Mean field theory.— The bosonization approach yields a good account of the overall structure of $P_{\tilde{t}}(w)$, but with certain limitations (see Fig. 2b). In particular, the assumption of a thermal final state is not quite correct. The occupation of the single particle levels after the time evolution is not described by the Fermi function but has a diffusive structure, as stated earlier. A more accurate expression can be obtained for $P_{\tilde{t}}(w)$ in a simple, particle number conserving *mean field* approach, where instead of assuming thermalization, we rely on the diffusive nature of energy absorption, and assume that each fermion level k is occupied with probability

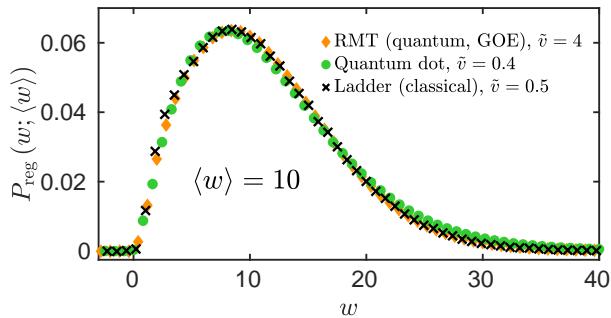


FIG. 3. Work statistics for dimensionless average work $\langle w \rangle = 10$. Microscopic quantum dot (QD) model simulations (green circles), random matrix (GOE) results (orange diamonds), and the ‘ladder’ model statistics (black crosses) fall on top of each other with good accuracy. QD calculations were performed for $M = 427$ electrons for a lattice of size 38×38 , disorder $D = 1.75J$, potential strength $\alpha = 75J$, and a dimensionless velocity, $\tilde{v} = 0.4$. For the GOE computations we used $N = 40$ with $M = 20$ electrons and a velocity $\tilde{v} = 4$. For the ‘ladder’ model simulations we used, $\tilde{v} = 0.5$ and $N = 120$ levels with $M = 60$ electrons. Quantum work distribution depends only on the average work $\langle w \rangle$ and is well captured by the classical ‘ladder’ model.

$f_k = (1 - \text{erf}[(\tilde{\epsilon}_k - \tilde{\epsilon}_F)/\sqrt{4\tilde{D}\tilde{t}}])/2$, corresponding to a diffusive broadening of the Fermi surface. To enforce the constraint, $\sum_k n_k = M$, we use an integral representation over an auxiliary variable. A saddle point procedure in this latter then yields accurate expressions for $P_{\text{ad}}(\tilde{t})$ as well as for $P_{\text{reg}}(w; \tilde{t})$.

The mean field probability distribution, $P_{\tilde{t}}^{\text{MF}}(w)$, is similar in structure to Eq. (6), but contains additional correction terms (see Ref. [31] for details),

$$P_{\tilde{t}}^{\text{MF}}(w) \approx P_{\text{ad}}^{\text{MF}} \delta(w) + \frac{c_w}{\sqrt{w}} e^{-c_w \frac{w + \langle w \rangle}{\sqrt{\langle w \rangle}}} \left[I_1(2c_w \sqrt{w}) - \sqrt{2} I_1(2c_w \sqrt{w/2}) \right] \quad (7)$$

with $c_w \approx 1.35$ and

$$P_{\text{ad}}^{\text{MF}} = (8\pi \langle w \rangle)^{1/4} e^{-c_w \sqrt{\langle w \rangle}}. \quad (8)$$

As shown in Fig. 2.b, the mean field expressions above yield an accurate description of work in the diffusive regime. Similar to the bosonization result, Eq. (6), $P_{\tilde{t}}^{\text{MF}}(w)$ is non-Gaussian and, by construction, depends parametrically only on $\langle w \rangle$. The probability of adiabatic processes also falls off as a stretched exponential, but the prefactor c_w is more accurate than the one obtained by the simple bosonization theory ($\pi/\sqrt{6} \approx 1.28$) [28, 31].

Validation by microscopic models and experimental setup.— To confirm the predictions above and to validate the results of our random matrix approach, we propose to study a 2-dimensional quantum dot (QD), and squeeze the electron gas confined there by applying time

dependent external gate voltages (see Fig. 1.a). This system can be realized experimentally [34, 35].

We model the QD by a disordered tight binding Hamiltonian,

$$H = -J \sum_{\mathbf{r}, \delta} c_{\mathbf{r}+\delta}^\dagger c_{\mathbf{r}} + \sum_{\mathbf{r}} (V(\mathbf{r}, t) + \epsilon_{\mathbf{r}}) c_{\mathbf{r}}^\dagger c_{\mathbf{r}}, \quad (9)$$

where the first term accounts for the kinetic energy of the electrons, while the potential $V(\mathbf{r}, t) = \frac{1}{2}(\alpha r^2 + \lambda(t)(x^2 - y^2))$ describes the parabolic confinement, generated by external gate electrodes. The second term in $V(\mathbf{r}, t)$ describes a compression (decompression) of the electron gas in the x direction with a simultaneous decompression (compression) along the y direction. We vary λ to induce deformations and generate dissipation. Finally, the random onsite energies $\epsilon_{\mathbf{r}}$ are drawn from a Gaussian distribution of variance, and are responsible for electron scattering and disorder.

A numerical investigation of the single particle spectrum of Eq. (9) reveals that, although some deviations are clearly present, the spectrum of Eq. (9) is reasonably described in terms of GOE for each value of λ (see Ref. [31]). We generate work then by varying λ uniformly in time, and use the determinant formula in Eq. (2) to compute $P_{\tilde{t}}(w)$. The disorder-averaged results for $P_{\text{reg}}(w; \tilde{t})$ are presented for $\langle w \rangle = 10$ in Fig. 3. They show striking agreement with random matrix theory as well as with the ‘ladder’ model, and thereby validate the latter.

An alternative experimental platform to study quantum work statistics is offered by ultracold atoms [12]. For a forward-backward protocol P_{ad} is essentially the ground state fidelity, which has been measured in Ref. [36] by preparing two identical copies of a quantum system, and measuring their overlap. This method could be used to verify the predicted stretched exponential behavior of P_{ad} in disordered fermion systems.

Conclusions.— We studied the full distribution of quantum work in disordered non-interacting fermion systems both within the framework of random matrix theory and in concrete microscopic model. Surprisingly, we found that for large enough average work, the distribution is independent of the random matrix ensemble and is very well captured by a classical stochastic model describing diffusion in energy space. This allowed us to make various simplifications (e.g. ‘ladder’ model) and derive approximate analytic expressions via bosonization and mean field theory. Interestingly, the bosonization result in Eq. (6) also emerged in the context of work statistics in Luttinger liquids after an interaction quench [16]. Let us stress that the final state is not thermal but has a diffusive occupation profile, which is the reason why the bosonization approach performs more poorly in comparison with the mean field treatment (cf. Fig. 2b). For an experimental realization, we propose

to study squeezed disordered quantum dots where our results could be tested experimentally.

Acknowledgments.— We thank Adolfo del Campo for interesting discussions. This work was supported by the National Research, Development and Innovation Office (NKFIH) through the Hungarian Quantum Technology National Excellence Program, project no. 2017-1.2.1-NKP-2017-00001, and by the ÚNKP-20-5 New National Excellence Program of the Ministry for Innovation and Technology. I. L. acknowledges support from the European Research Council (ERC) under the European Union’s Horizon 2020 research and innovation programme grant agreement No. 771537. M. K. was supported by a “Bolyai János” grant of the HAS.

-
- [1] M. Campisi, P. Hänggi, and P. Talkner, *Rev. Mod. Phys.* **83**, 771 (2011).
- [2] P. Talkner, E. Lutz, and P. Hänggi, *Phys. Rev. E* **75**, 050102(R) (2007).
- [3] S. Vinjanampathy and J. Anders, *Contemp. Phys.* **57**, 545 (2016).
- [4] J. Goold, M. Huber, A. Riera, L. del Rio, and P. Skrzypczyk, *J. Phys. A: Math. Theor.* **49**, 143001 (2016).
- [5] M. Campisi and J. Goold, *Phys. Rev. E* **95**, 062127 (2017).
- [6] A. Alemany, M. Ribezzi, and F. Ritort, *AIP Conf. Proc.* **1332**, 96 (2011).
- [7] J. Liphardt, S. Dumont, S. B. Smith, I. Tinoco Jr., C. Bustamante, *Science* **96**, 1833 (2002).
- [8] D. Collin, F. Ritort, C. Jarzynski, S. B. Smith, I. Tinoco Jr., and C. Bustamante, *Nature* **437**, 231 (2005).
- [9] O.-P. Saira, Y. Yoon, T. Tanttu, M. Möttönen, D. V. Averin, and J. P. Pekola, *Phys. Rev. Lett.* **109**, 180601 (2012).
- [10] J. V. Koski and J. P. Pekola, in: Binder F., Correa L., Gogolin C., Anders J., Adesso G. (eds), *Thermodynamics in the Quantum Regime*, Fundamental Theories of Physics, vol 195. Springer, Cham
- [11] T. B. Batalhão, A. M. Souza, L. Mazzola, R. Aucaisse, R. S. Sarthour, I. S. Oliveira, J. Goold, G. De Chiara, M. Paternostro, and R. M. Serra, *Phys. Rev. Lett.* **113**, 140601 (2014).
- [12] Federico Cerisola, Yair Margalit, Shimon Machluf, Augusto J Roncaglia, Juan Pablo Paz, and Ron Folman, *Nat. Commun.* **8**, 1241 (2017).
- [13] J. Klatzow, J. N. Becker, P. M. Ledingham, C. Weinzetl, K. T. Kaczmarek, D. J. Saunders, J. Nunn, I. A. Walmsley, R. Uzdin, and E. Poem, *Phys. Rev. Lett.* **122**, 110601 (2019).
- [14] A. Silva, *Phys. Rev. Lett.* **101**, 120603 (2008).
- [15] A. Gambassi, and A. Silva, *Phys. Rev. Lett.* **109**, 250602 (2012).
- [16] B. Dóra, Á. Bácsi, and G. Zaránd, *Phys. Rev. B* **86**, 161109(R) (2012).
- [17] S. Dorosz, T. Platini, and D. Karevski, *Phys. Rev. E* **77**, 051120 (2008).
- [18] J. Yi, P. Talkner, and M. Campisi, *Phys. Rev. E* **84**, 011138 (2011).
- [19] J. Yi, Y. W. Kim, and P. Talkner, *Phys. Rev. E* **85**, 051107 (2012).
- [20] G. Perfetto, L. Piroli, and A. Gambassi, *Phys. Rev. E* **100**, 032114 (2019).
- [21] A. Chenu, I. L. Egusquiza, J. Molina-Vilaplana, and A. del Campo, *Sci. Rep.* **8**, 12634 (2018).
- [22] M. Łobejko, J. Luczka, and P. Talkner, *Phys. Rev. E* **95**, 052137 (2017).
- [23] E. G. Arrais, D. A. Wisniacki, L. C. Céleri, N. G. de Almeida, A. J. Roncaglia, and F. Toscano, *Phys. Rev. E* **98**, 012106 (2018).
- [24] A. Chenu, J. Molina-Vilaplana, and A. del Campo, *Quantum* **3**, 127 (2019).
- [25] C. W. J. Beenakker, *Rev. Mod. Phys.* **69**, 731 (1997).
- [26] T. Guhr, A. Müller-Groeling, and H. A. Weidenmüller, *Phys. Rep.* **299**, 189 (1998).
- [27] P. N. Walker, M. J. Sánchez, and M. Wilkinson, *J. Math. Phys.* **37**, 5019 (1996).
- [28] I. Lovas, A. Grabarits, M. Kormos, and G. Zaránd, *Phys. Rev. Research* **2**, 023224 (2020).
- [29] A. Grabarits, I. Lovas, M. Kormos, and G. Zaránd, *in preparation*.
- [30] A similar determinant formula has been derived in a parallel work, Z. Fei and H. T. Quan, *Phys. Rev. Research* **1**, 033175 (2019).
- [31] Supplemental Material containing details of the bosonization and mean field calculations, and additional plots about energy space diffusion and the level spacing distribution of the microscopic 2D quantum dot system.
- [32] For $N \times N$ random matrices, $\delta\epsilon \sim 1/N$, and $\langle \Delta\lambda \rangle \sim 1/\sqrt{N}$, therefore $v_c \sim 1/N^{3/2}$.
- [33] J. von Delft and H. Schoeller, *Ann. Phys.* **7**, 225 (1998).
- [34] S. Gasparinetti, K. L. Viisanen, O. P. Saira, T. Faivre, M. Arzeo, M. Meschke, and J.P. Pekola, *Phys. Rev. Applied* **3**, 014007 (2015).
- [35] E. D. Walsh, D. K. Efetov, G.-H. Lee, M. Heuck, J. Crossno, T. A. Ohki, P. Kim, D. Englund, and K. C. Fong, *Phys. Rev. Applied* **8**, 024022 (2017).
- [36] A. M. Kaufman, M. E. Tai, A. Lukin, M. Rispoli, R. Schittko, P. M. Preiss, M. Greiner, *Science* **353**, 794 (2016).

SUPPLEMENTARY MATERIAL

BOSONIZATION APPROACH

In this approach, we consider an equilibrium fermionic system with uniformly spaced one-particle energy levels. In the framework of bosonization, the fermionic particle-hole excitations with respect to the ground state are represented as bosonic states. We assign thermal Boltzmann weights $e^{-\beta_{\text{eff}} q \delta \varepsilon}$ to these states, where β_{eff} is an effective inverse temperature while $q \delta \varepsilon$ with $q = 1, 2, \dots$ measures the energy of the particle-hole excitation. Since these excitations are bosonic, for each q we can have $n_q = 0, 1, 2, \dots$ arbitrarily many bosonic excitations with energy $q n_q \delta \varepsilon$. In the characteristic function each of them carries a contribution of $e^{i \tilde{u} q n_q}$, so we have

$$\begin{aligned} G_t^{\text{Bose}}(u) &= \mathcal{N}^{-1} \sum_{n_1, n_2, \dots} e^{-(\beta_{\text{eff}} \delta \varepsilon - i \tilde{u}) n_1} e^{-(\beta_{\text{eff}} \delta \varepsilon - i \tilde{u}) 2 n_2} e^{-(\beta_{\text{eff}} \delta \varepsilon - i \tilde{u}) 3 n_3} \dots = \mathcal{N}^{-1} \prod_{q=1}^{\infty} \sum_{n_q=0}^{\infty} e^{-q n_q (\beta_{\text{eff}} \delta \varepsilon - i \tilde{u})} \\ &= \mathcal{N}^{-1} \prod_{q>0} \frac{1}{1 - e^{-q(\beta_{\text{eff}} \delta \varepsilon - i \tilde{u})}}, \end{aligned} \quad (10)$$

where $\mathcal{N} = \prod_{q>0} [1 - e^{-q(\beta_{\text{eff}} \delta \varepsilon)}]^{-1}$ so that $G_{\text{eff}}(0, T_{\text{eff}}) = 1$. Exponentiating Eq. (10) and taking the continuum limit $\sum_{q>0} \rightarrow \int_0^{\infty} dx$ we get:

$$G_t^{\text{Bose}}(u) \approx \mathcal{N}^{-1} e^{-\int_0^{\infty} dx \ln [1 - e^{-(\beta_{\text{eff}} - i u)x}]} = e^{\frac{\pi^2/6}{\beta_{\text{eff}} - i u} - \frac{\pi^2/6}{\beta_{\text{eff}}}}. \quad (11)$$

The Fourier transform can be computed analogously to the the mean field treatment above with the result

$$P_t^{\text{Bose}}(w) \approx e^{-\frac{\pi^2}{6\beta_{\text{eff}}}} \left[\frac{\pi}{\sqrt{6}} e^{-\beta_{\text{eff}} w} \frac{I_1\left(\pi \sqrt{\frac{2}{3}} w\right)}{\sqrt{w}} + \delta(w) \right]. \quad (12)$$

MEAN FIELD APPROACH

In this section we provide some details about the mean field theory calculations and the resulting analytic expressions.

Probability of adiabaticity

Within the mean field approach, the probability of each many-body configuration takes the form of the product of independent Bernoulli weights of M occupied and $N - M$ empty sites. In order to simplify calculations and without any loss of generality we consider the case of $M = N/2$:

$$\begin{aligned} P(\{n_k\}) &= \frac{1}{\mathcal{N}_t} \prod_{k=1}^N p_{k,t}(n_k) \delta_{N/2 = \sum_k n_k} \\ &= \frac{1}{\mathcal{N}_t} \int_{-\pi}^{\pi} \frac{d\lambda}{2\pi} e^{i\lambda \sum_{k=1}^N (n_k - 1/2)} \prod_{k=1}^N p_{k,t}(n_k), \end{aligned} \quad (13)$$

where the particle number conservation is taken into account by the Kronecker-delta for which we used a standard integral representation. The Bernoulli weights are

$$p_{k,t}(n_k) = n_k f_k(t) + (1 - n_k)(1 - f_k(t)), \quad (14)$$

where $f_k(t) = (1 - t_k(t))/2$ with $t_k(t) = \text{erf}(\Delta k/\sqrt{4\tilde{D}t})$ and $\Delta k = k - M - 1/2$ is measured from the Fermi-level. Finally, the time-dependent normalization factor is the sum of all possible many-body probabilities:

$$\begin{aligned} \mathcal{N}_t &\equiv \sum_{\{n_k\}} P(\{n_k\}) = \int_{-\pi}^{\pi} \frac{d\lambda}{2\pi} \prod_{k=1}^N \left[e^{i\lambda/2} f_k(t) + e^{-i\lambda/2} (1 - f_k(t)) \right] = \int_{-\pi}^{\pi} \frac{d\lambda}{2\pi} \prod_{k=1}^N [\cos(\lambda/2) - i \sin(\lambda/2) t_k(t)] \\ &= \int_{-\pi}^{\pi} \frac{d\lambda}{2\pi} \prod_{\Delta k > 0} [\cos^2(\lambda/2) + \sin^2(\lambda/2) t_k(t)]. \end{aligned} \quad (15)$$

Writing the above expression as the exponential of its logarithm, approximating the resulting sum by an integral and performing a saddle point approximation around $\lambda = 0$, we obtain for large enough values of $\langle w \rangle = \tilde{D}t \gg 1$:

$$\begin{aligned} \mathcal{N}_t &\approx \int_{-\pi}^{\pi} \frac{d\lambda}{2\pi} \exp \left[\int_0^{\infty} dx \log(\cos^2 \lambda/2 + t_x(t) \sin^2 \lambda/2) \right] \\ &\approx \int_{-\pi}^{\pi} \frac{d\lambda}{2\pi} \exp \left[- \int_0^{\infty} dx \lambda^2/4(1 - t_x(t)) \right] = (8\pi \langle w \rangle)^{-1/4}. \end{aligned} \quad (16)$$

The probability of adiabaticity then reads

$$\begin{aligned} P_{\text{ad}}(\tilde{t}) &= \frac{1}{\mathcal{N}_t} \prod_{\Delta k < 0} f_k(t) \prod_{\Delta k > 0} (1 - f_k(t)) \\ &\approx \frac{1}{\mathcal{N}_t} e^{2\sqrt{4\langle w \rangle} \int_0^{\infty} dx \log[(1 + \text{erf}(x))/2]} = (8\pi \tilde{D}t)^{1/4} e^{-C\sqrt{\tilde{D}t}} = (8\pi \langle w \rangle)^{1/4} e^{-C\sqrt{\langle w \rangle}} \end{aligned}$$

with $C \approx 1.35$.

Variance of work

For $\langle w \rangle \gg 1$, we approximate the variance of the work by neglecting the fluctuations of the energy levels [1], $\varepsilon_k(t) \rightarrow \Delta k \delta\varepsilon$, but incorporating the fluctuations of the occupation numbers. For a given realization of $\mathcal{H}(t)$, this leads to the estimate

$$\delta w^2(t) \approx \left\langle \left(\sum_{k=1}^N \Delta k \hat{n}_{k,t} \right)^2 \right\rangle - \left\langle \sum_{k=1}^N \Delta k \hat{n}_{k,t} \right\rangle^2,$$

where $\langle \dots \rangle$ denotes quantum average. Separating the diagonal terms, the RM average $\langle \delta w^2(t) \rangle_{\text{RM}}$ can be written as

$$\langle \delta w^2(t) \rangle_{\text{RM}} \approx \sum_k \Delta k^2 \langle \langle \delta \hat{n}_{k,t}^2 \rangle \rangle_{\text{RM}} + \sum_{k \neq k'} \Delta k \Delta k' \langle \langle \delta \hat{n}_{k,t} \delta \hat{n}_{k',t} \rangle \rangle_{\text{RM}}, \quad (17)$$

where $\delta \hat{n}_{k,t} \equiv \hat{n}_{k,t} - \langle \hat{n}_{k,t} \rangle$ is the deviation of the occupation number from the mean value. As the $\hat{n}_{k,t}$ behave as binary random variables, the averages in the first term are given by $\langle \langle \delta \hat{n}_{k,t}^2 \rangle \rangle_{\text{RM}} = f_k(t)(1 - f_k(t))$. The correlators in this equation can be expressed in terms of the amplitudes $\alpha_k^m(t)$ as $\langle \delta \hat{n}_{k,t} \delta \hat{n}_{k',t} \rangle = -|\sum_{m=1}^{N/2} \alpha_k^m(t)^* \alpha_{k'}^m(t)|^2$. The negativity of this correction implies that the level occupations are *anticorrelated*, as follows from particle number conservation.

Neglecting this correction for the moment and replacing sums by integrals, we arrive at the estimate

$$\langle \delta w^2(t) \rangle_{\text{RM}} \approx \int_{-\infty}^{\infty} dx x^2 \frac{1 - \text{erf}^2(x/\sqrt{4\tilde{D}t})}{4} \sim \tilde{t}^{3/2},$$

yielding $\langle \delta w^2(t) \rangle \sim \langle w \rangle^{3/2}$. We thus recovered the observed behavior, however, the prefactor turns out to be incorrect. A more careful mean field calculation shows that the occupation number correlations (related to fermion number conservation) cannot be neglected but they also turn out to give a (smaller) $\sim \tilde{t}^{3/2}$ contribution, thus altering the prefactor but keeping the overall scaling the same.

Distribution of work

The characteristic function of the distribution of work can be expressed as

$$\begin{aligned}
G_t^{\text{MF}}(u) &= \left\langle e^{iu \sum_k \Delta k \delta \varepsilon n_k} \right\rangle_{\text{MF}} e^{-iu E_{\text{GS}}} = \sum_{\{n_k\}} P_{\{n_k\}} e^{i\tilde{u} \sum_k \Delta k (n_k - 1/2)} \\
&= \frac{1}{\tilde{\mathcal{N}}_t} \int_{-\pi}^{\pi} \frac{d\lambda}{2\pi} \prod_{\Delta k} \left[e^{i(\lambda + \tilde{u}\Delta k)/2} f_k(t) + e^{-i(\lambda + \tilde{u}\Delta k)/2} f_{-k}(t) \right] \\
&= \frac{1}{\tilde{\mathcal{N}}_t} \int_{-\pi}^{\pi} \frac{d\lambda}{2\pi} \prod_{\Delta k < 0} \left[f_k(t) + e^{-i(\lambda + \tilde{u}\Delta k)} f_{-k}(t) \right] \prod_{\Delta k > 0} \left[f_{-k}(t) + e^{i(\lambda + \tilde{u}\Delta k)} f_k(t) \right] \\
&\approx \frac{1}{\tilde{\mathcal{N}}_t} \int_{-\pi}^{\pi} \frac{d\lambda}{2\pi} \exp \left[\int_0^\infty dx \ln (1 + h_x^2(u, t) + 2h_x(u, t) \cos(\lambda)) \right],
\end{aligned} \tag{18}$$

where we introduced the scaled variable $\tilde{u} = u \delta \varepsilon$ and the notation $h_k(u, t) = \frac{f_k(t)}{f_{-k}(t)} e^{i\tilde{u}\Delta k}$. Here $\langle \dots \rangle_{\text{MF}}$ denotes averaging over the mean field many-body probabilities and $\tilde{\mathcal{N}}_t$ a modified normalization constant. As numerics revealed, for large enough injected works $\langle w \rangle \gg 1$ neglecting particle number conservation does not introduce big errors provided we subtract the pure particle-hole excitations with respect to the ground state:

$$G_t^{\text{MF}}(u) \approx \frac{1}{\tilde{\mathcal{N}}_t} \left\{ e^{2 \int_0^\infty dx \ln(1+h_x(t,u))} - 2 \left[e^{\int_0^\infty dx \ln(1+h_x(t,u))} - 1 \right] \right\}, \tag{19}$$

where the first term is the $\lambda = 0$ saddle-point solution of the integral expression, while the second part subtracts the contributions coming from the pure particle-hole excitations. Here the integrals can be approximated as

$$2 \int_0^\infty dx \ln [1 + h_x(u, t)] \approx \frac{c_w^2}{\sqrt{\langle w \rangle} - iu} \tag{20}$$

yielding

$$G_t^{\text{MF}}(u) \approx \frac{1}{\tilde{\mathcal{N}}_t} \left\{ e^{\frac{c_w^2}{\sqrt{\langle w \rangle} - iu}} - 2 \left[e^{\frac{c_w^2/2}{\sqrt{\langle w \rangle} - iu}} - 1 \right] \right\} \tag{21}$$

with $c_w = \frac{3\sqrt{2\pi}}{5}$ chosen such that the characteristic function correctly reproduces the first two cumulants of work in the saddle point solution. Now this expression can be Fourier transformed exactly as

$$\begin{aligned}
\int_{-\infty}^{\infty} \frac{du}{2\pi} e^{-iuw} e^{\frac{c_w^2}{\sqrt{\langle w \rangle} - iu}} &= \sum_{n=0}^{\infty} \frac{c_w^{2n}}{n!} \int_{-\infty}^{\infty} \frac{du}{2\pi} \frac{e^{-iuw}}{\left(\frac{c_w}{\sqrt{\langle w \rangle}} - iu \right)^n} = e^{-\frac{c_w}{\sqrt{\langle w \rangle}} w} \sum_{n=1}^{\infty} \frac{c_w^{2n} w^{n-1}}{n!(n-1)!} + \delta(w) \\
&= e^{-\frac{c_w}{\sqrt{\langle w \rangle}} w} c_w \frac{I_1(2c_w \sqrt{w})}{\sqrt{w}} + \delta(w)
\end{aligned} \tag{22}$$

which leads to the approximate analytic expression

$$P_t^{\text{MF}}(w) \approx e^{-c_w \sqrt{\langle w \rangle}} \left[e^{-\frac{c_w}{\sqrt{\langle w \rangle}} w} c_w \left(\frac{I_1(2c_w \sqrt{w})}{\sqrt{w}} - \frac{I_1(2c_w \sqrt{w/2})}{\sqrt{w/2}} \right) + \delta(w) \right]. \tag{23}$$

ENERGY SPACE DIFFUSION

In this section we demonstrate that the energy level occupations exhibit a diffusive profile, meaning that particle-hole excitations happen dominantly in a window growing as $\sim \langle w \rangle^{1/2}$, for all the random matrix ensembles as well as for the ‘‘ladder model’’ and the disordered quantum dot. The left panel of Fig. 4 shows that for large enough average

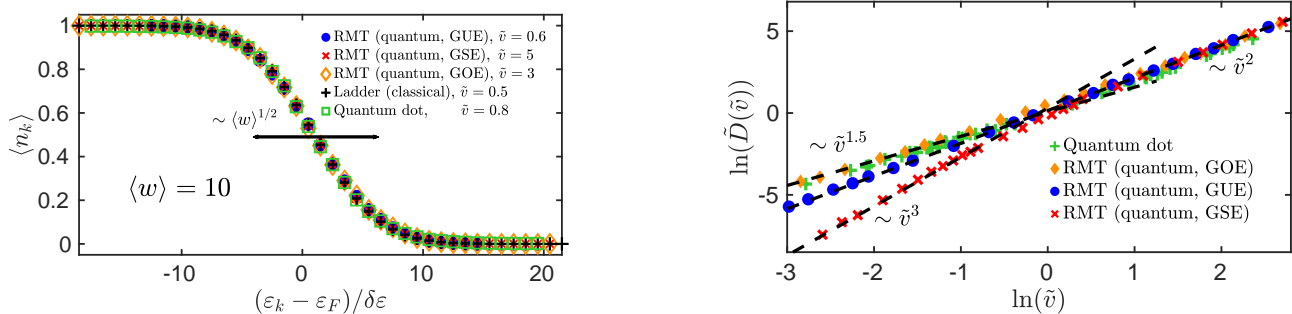


FIG. 4. Energy space diffusion. *Left*: Average occupations of instantaneous single particle eigenstates for the three RMT ensembles (GOE, GUE, GSE) and the quantum dot model compared to the classically obtained results within the ladder model. All the five curves collapse onto a single universal, diffusively broadening profile given by $\left[1 - \operatorname{erf}\left(\Delta k/\sqrt{4\langle w \rangle}\right)\right]/2$. *Right*: Velocity dependence of the diffusion constant. For slow quenches it has an anomalous power-law behavior, $\tilde{D}(\tilde{\nu} \lesssim 1) \sim \tilde{\nu}^{\beta/2+1}$, while for fast quenches it grows quadratically and with the same prefactor for the RMT ensembles. The quantum dot displays a similar behavior as the GOE ensemble in the two limiting cases, with a slightly different prefactor.

work the mean level occupation for of all three RMT ensembles (GOE, GUE, GSE) follows a single universal curve identical to those of the quantum dot model up to high precision and it is also perfectly described by the ladder model. Numerical calculations were made for $\sim 5 \times 10^3$ disorder realizations both for RMT and the disordered quantum dot, for $N = 40, 28, 40$ for the three ensembles, respectively and for parameters $L = 38, \sigma = 1.75J, \alpha = 75J$ and with 427 particles in the case of the quantum dot.

The right panel of Fig. 4 shows the velocity dependence of the diffusion constant, $\tilde{D}_\beta(\tilde{\nu})$ for the three ensembles and the quantum dot model. We averaged over $\sim 5 \times 10^3$ simulations, yielding smooth enough time-evolutions of average work to extract the diffusion constants. Parameters were chosen such that we avoid finite size effects and be in the diffusion regime. The rate of energy absorbed by the system exhibits an anomalous frequency dependence for slow quenches, $\tilde{D}_\beta(\tilde{\nu} \lesssim 1) \sim \tilde{\nu}^{\beta/2+1}$, while for fast processes becomes independent of the underlying symmetry class and grows quadratically, as it should in the case of a metal, $\tilde{D}_\beta(\tilde{\nu} \gg 1) \sim \tilde{\nu}^2$. The diffusion constant for the quantum dot shows the same power-law behavior as the GOE ensemble, albeit with a slightly smaller prefactor.

Finally, we compare the level spacing distribution of the GOE ensemble and the disordered quantum dot. As shown in Fig. 5, the distribution of the distance of neighboring levels are well described by the analytical RMT result given by the Wigner surmise. Similar observations hold for the statistics of the the Landau-Zener parameters at the avoided level crossings in comparison with the RMT results of Ref. [2].

[1] W. B. Thimm, J. Kroha, and J. von Delft, Phys. Rev. Lett. **82**, 2143 (1999).

[2] P. N. Walker, M. J. Sánchez, and M. Wilkinson, J. Math. Phys. **37**, 5019 (1996).

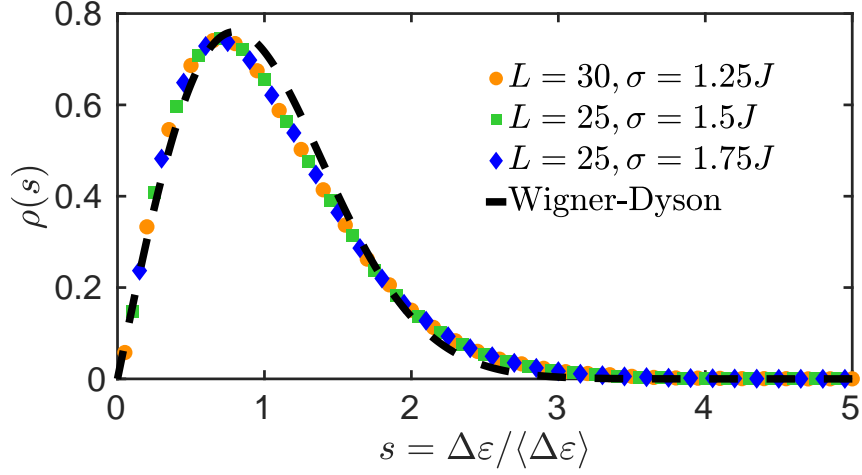


FIG. 5. Distribution of the distance between neighboring levels in the middle of the spectrum, $\Delta\varepsilon \equiv \varepsilon_{L^2/2+1} - \varepsilon_{L^2/2}$, normalized to unit mean, for the quantum dot at three different set of parameters, $L = 30, \sigma = 1.25J$, $L = 25, \sigma = 1.5J$, $L = 25, \sigma = 1.75J$ for the orange circles, green squares and blue diamonds, respectively. The potential strength is kept fixed, $\alpha = 70J$ for all the three curves. The dashed line indicates the well-known Wigner–Dyson result, $\rho(s) \approx \frac{\pi}{2} s e^{-\frac{\pi}{4}s^2}$, obtained by Wigner’s surmise describing the GOE case. For the numerical calculations we averaged over $\sim 5 \times 10^4$ disorder realizations which proved to yield smooth enough curves.